Forward–backward emission of target evaporated fragments in high energy nucleus–nucleus collisions *

ZHANG Zhi(张智) MA Tian-Li(马田丽) ZHANG Dong-Hai(张东海)[1)]

Institute of Modern Physics, Shanxi Normal University, Linfen 041004, China

Abstract: The multiplicity distribution, multiplicity moment, scaled variance, entropy and reduced entropy of target evaporated fragments emitted in forward and backward hemispheres in 12 A GeV ^{4}He, 3.7 A GeV ^{16}O, 60 A GeV ^{16}O, 1.7 A GeV ^{84}Kr and 10.7 A GeV ^{197}Au -induced emulsion heavy target (AgBr) interactions are investigated. It is found that the multiplicity distribution of target evaporated fragments emitted in both forward and backward hemispheres can be fitted by a Gaussian distribution. The multiplicity moments of target evaporated particles emitted in the forward and backward hemispheres increase with the order of the moment q, and the second-order multiplicity moment is energy independent over the entire energy range for all the interactions in the forward and backward hemisphere. The scaled variance, a direct measure of multiplicity fluctuations, is close to one for all the interactions, which indicate a correlation among the produced particles. The entropy of target evaporated fragments emitted in both forward and backward hemispheres are the same within experimental errors.

Key words: relativistic heavy-ion collisions, target fragmentation, multiplicity, nuclear emulsion

PACS: 25.75.-q, 25.70.Mn, 25.75.Ag **DOI:** 10.1088/1674-1137/39/10/104002

1 Introduction

In high energy nucleus–nucleus collisions, the multiplicity is an important variable which can help to test different phenomenological and theoretical models and to understand the mechanism of multi-particle production. According to the participant–spectator model [1], three different types of secondary particles, projectile fragments, target fragments and produced particles are produced in high energy nucleus–nucleus collisions. The produced particles are single-charged relativistic particles having velocity $v \geqslant 0.7\ c$. Most of them are pions, contaminated with small proportions of fast protons and K mesons. The multiplicity of produced particles has been studied exclusively because they carry the essential information of the interaction mechanism. The projectile fragments are the decayed particles of the excited projectile residues through evaporation of neutrons and light nuclei, and it has been speculated that the decay of highly excited nuclear matter systems may carry information about the equation of state and the liquid–gas phase transition of low-density nuclear matter. The target fragments include target recoil protons and target evaporated fragments. The target recoil protons are formed due to fast target protons of energy ranging up to 400 MeV. The target evaporated particles are of low-energy (<30 MeV) singly or multiply charged fragments. In emulsion terminology [2], the target recoiled particles are referred to as "grey track particles" and the target evaporated particles are referred to as "black track particles". According to the cascade evaporation model [2], the grey track particles are emitted from the nucleus very soon after the instant of impact, leaving the hot residual nucleus in an excited state. The emission of black track particles from this state takes place relatively slowly. In the rest system of the target nucleus, the emission of evaporated particles is assumed to be isotropic over the whole phase space. Much attention has been paid to investigate the production of grey track particles because it is believed to be a quantitative probe of intranuclear cascading collisions. Little attention has been paid to the study of the production of black particles, because these particles are emitted at a late stage of nuclear interactions. However, the study of target evaporated particles is also important because they are expected to remember the history of the interactions. Hence, the emission of these particles may also be of physical interest.

The emission of target evaporated fragments is isotropic in the rest system of the target nucleus according to the cascade evaporation model, but because of the

Received 5 January 2015

∗ Supported by National Science Foundation of China (11075100), Natural Science Foundation of Shanxi Province (2011011001-2) and the Shanxi Provincial Foundation for Returned Overseas Chinese Scholars, (2011-058)

1) E-mail: zhangdh@dns.sxnu.edu.cn

electromagnetic field from the projectile, this isotropic emission property may be distorted. It is therefore necessary to compare the emission properties of target evaporated fragments in the forward hemisphere (emission angle $\theta_{\rm Lab}\leqslant 90^\circ$) and in the backward hemisphere (emission angle $\theta_{\rm Lab}>90^\circ$). If the nature of multiplicity distribution in the forward and backward hemispheres is similar, then isotropic target evaporated fragment emission may be assumed. If, on the other hand, the multiplicity distributions in the two hemispheres are different, then the emission mechanism of target evaporated fragments in the forward and backward hemispheres may be different. This could be interesting and deserves the attention of the physics community.

Ghosh et al. [3] studied the emission properties of target evaporated fragments in the forward and backward hemispheres produced in 3.7 A GeV ^{12}C-AgBr, 14.5 A GeV ^{28}Si-AgBr, 60 A GeV ^{16}O-AgBr and 200 A GeV ^{32}S-AgBr interactions, and a difference in multiplicity distribution was found in the forward and backward hemispheres. In our recent paper [4] the forward–backward correlations for target fragments emitted in 150 A MeV ^{4}He-AgBr, 290 A MeV ^{12}C-AgBr, 400 A MeV ^{12}C-AgBr, 400 A MeV ^{20}Ne-AgBr and 500 A MeV ^{56}Fe-AgBr interactions were studied.

In this paper, the production of target evaporated fragments emitted from 12 A GeV ^{4}He-AgBr, 3.7 A GeV ^{16}O-AgBr, 60 A GeV ^{16}O-AgBr, 1.7 A GeV ^{84}Kr-AgBr and 10.7 A GeV ^{197}Au-AgBr interactions are investigated. The multiplicity distribution, multiplicity moments, scaled variance, entropy and reduced entropy of target evaporated fragments emitted in forward and backward hemispheres are discussed respectively.

2 Experimental details

Five nuclear emulsion stacks, provided by the EMU01 Collaboration, were used in the present investigation. The stacks were exposed horizontally to 12 A GeV ^{4}He, 3.7 A GeV ^{16}O, 60 A GeV ^{16}O, 1.7 A GeV ^{84}Kr and 10.7 A GeV ^{197}Au. BA2000 and XSJ-2 microscopes with a 100× oil immersion objective and 10× ocular lenses were used to scan the plates. The tracks were picked up at a distance of 5 mm from the edge of the plates and they were carefully followed until they either interacted with emulsion nuclei or escaped from the plates. Interactions within 30 μm of the top or bottom surface of the emulsion plates were not considered for final analysis. In each interaction all of the secondaries were recorded, including shower particles, target recoiled protons, target evaporated fragments and projectile fragments. Details of track scanning and track classification can be found in our paper [4].

The nuclear emulsion is composed of a homogeneous mixture of H, C, N, O, S, I, Br, and Ag nuclei, and the major composition is H, C, N, O, Br, and Ag. According to the value of $n_{\rm h}$ (multiplicity of the target recoiled protons and evaporated fragments) the interactions are divided into the following three groups. Events with $n_{\rm h}\leqslant 1$ are due to interactions with H target and peripheral interactions with CNO and AgBr targets, events with $2\leqslant n_{\rm h}\leqslant 7$ are due to interactions with CNO targets and peripheral interactions with AgBr targets, and events with $n_{\rm h}\geqslant 8$ definitely belong to interactions with AgBr targets.

To ensure the targets in the nuclear emulsion are silver or bromine nuclei, we have chosen only the events with at least eight heavy ionizing track particles.

3 Results and discussion

The general characteristics of 12 A GeV ^{4}He, 3.7 A GeV ^{16}O, 60 A GeV ^{16}O, 1.7 A GeV ^{84}Kr and 10.7 A GeV ^{197}Au -induced AgBr interactions, including event statistics, average multiplicity of the target evaporated fragments emitted in forward hemisphere ($\langle n_{\rm b}^{\rm f}\rangle$), backward hemisphere ($\langle n_{\rm b}^{\rm b}\rangle$) and whole space ($\langle n_{\rm b}\rangle$), are presented in Table 1. It is found that the proportion of target evaporated fragments emitted in the forward hemisphere is greater than in the backward hemisphere.

Figures 1 to 5 show the multiplicity distributions of target evaporated fragments emitted in the forward hemisphere, backward hemisphere and the whole space. It is found that the distributions can be well fitted by a Gaussian distribution for 3.7 A GeV ^{16}O, 60 A GeV ^{16}O, 1.7 A GeV ^{84}Kr and 10.7 A GeV ^{197}Au -induced AgBr interactions, but for 12 A GeV ^{4}He -induced AgBr target interactions the distributions can be fitted by the superposition of two Gaussian distributions. The Gaussian fitting parameters (mean value and error) and χ^2/DOF are presented in Table 2, where DOF means the degree

Table 1. Average multiplicity of target evaporated fragments in the forward and backward hemispheres for different nucleus-AgBr interactions.

beam	number of events	$\langle n_{\rm b}^{\rm f}\rangle$	$\langle n_{\rm b}^{\rm b}\rangle$	$\langle n_{\rm b}\rangle$
12 A GeV He	2975	4.62±0.05	3.65±0.04	8.26±0.08
3.7 A GeV O	927	6.04±0.11	4.47±0.08	10.50±0.16
60 A GeV O	521	5.98±0.12	5.12±0.11	11.05±0.19
1.7 A GeV Kr	229	6.27±0.21	4.07±0.15	10.34±0.29
10.7 A GeV Au	619	5.01±0.11	3.66±0.09	8.67±0.17

Table 2. Gaussian fitting parameters of target evaporated fragment multiplicity distributions in the forward and backward hemispheres for different type of nucleus-AgBr interactions.

beam	forward hemisphere			backward hemisphere			whole space			reference
	mean value	error	χ^2	mean value	error	χ^2	mean value	error	χ^2	
12 A GeV He	2.80±0.11	1.49±0.13	1.57	2.59±0.16	1.76±0.18	2.97	5.38±0.15	2.19±0.11	2.72	this work
	5.68±0.41	3.03±0.15		4.94±1.18	2.69±0.30		10.69±0.37	4.38±0.16		this work
3.7 A GeV O	5.79±0.12	3.23±0.10	1.47	4.20±0.10	2.64±0.09	0.60	10.40±0.17	4.81±0.14	1.17	this work
60 A GeV O	5.79±0.13	2.65±0.11	2.59	5.08±0.11	2.43±0.08	1.56	10.74±0.19	4.05±0.15	1.31	this work
1.7 A GeV Kr	6.18±0.20	2.76±0.16	1.47	3.82±0.18	2.36±0.18	0.64	9.87±0.30	4.12±0.27	0.83	this work
10.7 A GeV Au	4.72±0.13	2.84±0.12	1.07	3.27±0.12	2.50±0.11	1.03	8.44±0.19	4.37±0.20	0.60	this work
3.7 A GeV C	5.00	3.26	0.51	4.57	2.80	0.48				[3]
14.5 A GeV Si	5.27	2.13	0.32	4.27	1.93	0.87				[3]
60 A GeV O	7.19	2.93	0.54	4.53	2.99	0.29				[3]
200 A GeV S	4.78	4.46	0.68	3.89	2.80	0.61				[3]

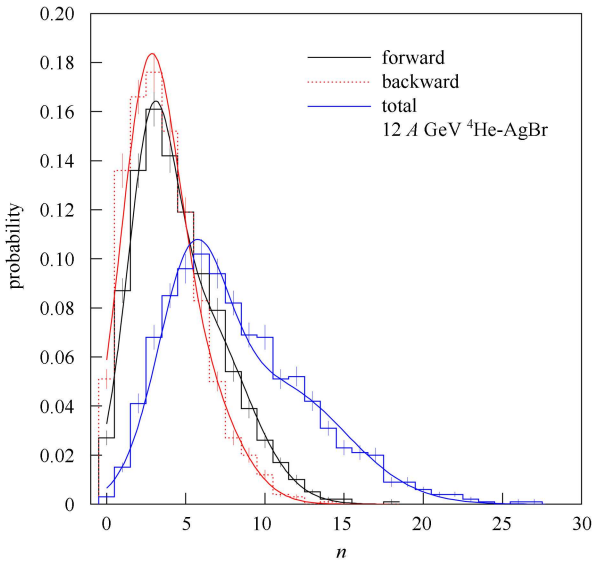

Fig. 1. (color online) Multiplicity distributions of target evaporated fragments emitted in 12 A GeV ^{4}He-AgBr interactions; the smooth curves are the results from the Gaussian fitting.

of freedom of simulation. For comparison the results in Ref. [3] are also included in the table. It is found that the fitting parameters are different between the forward and backward hemispheres for all the interactions, and the mean values and errors of Gaussian distributions in the forward hemisphere are greater than in the backward hemisphere. The difference in the nature of multiplicity distributions between the two hemispheres may be attributed to the fact that the mechanism of the target fragmentation process is different in the forward and backward hemispheres. Based on the cascade evaporation model [2], the emission of the target evaporated fragments should be isotropic in the laboratory frame, but due to the electromagnetic field from the projectile, the emission of target evaporated fragments is close to $\theta_{\rm Lab} \approx 90^\circ$ symmetric and the emission probability in the forward hemisphere is greater than that in the backward hemisphere. According to the model proposed by Stocker et al. [5] using three-dimensional nuclear fluid dynamics, the emission of target fragments in the backward hemisphere can be explained with the help of the side splash phenomenon. In a nucleus–nucleus collision, a head shock zone may be developed during the dividing phase of the projectile nucleus with the target. A strongly compressed and highly excited projectile-like object continues to interpenetrate the target with supersonic velocity and may push the matter sideways. This results in the generation of shock waves that give rise to particle evaporation in the backward directions. At intermediate impact parameters the highly inelastic bounce-off appears, where the large compression potential leads to the sideways deflection of the projectile, which then explodes. A large collective transverse momentum transfer to the target leads to azimuthally asymmetric fragment distribution.

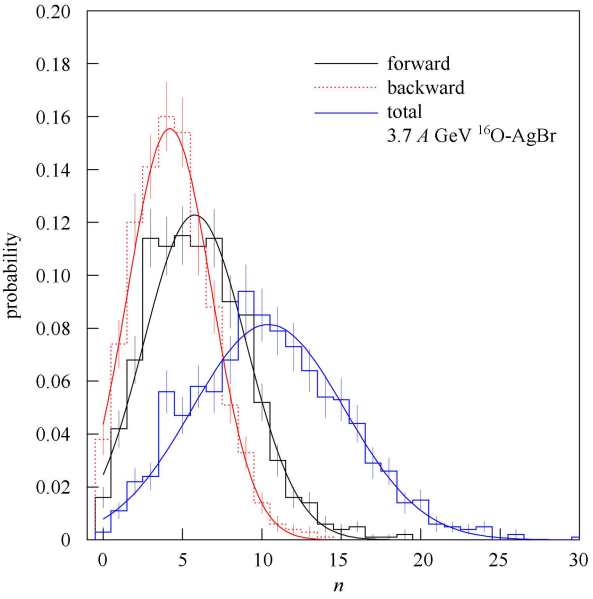

Fig. 2. (color online) Multiplicity distributions of target evaporated fragments emitted in 3.7 A GeV ^{16}O-AgBr interactions; the smooth curves are the results from the Gaussian fitting.

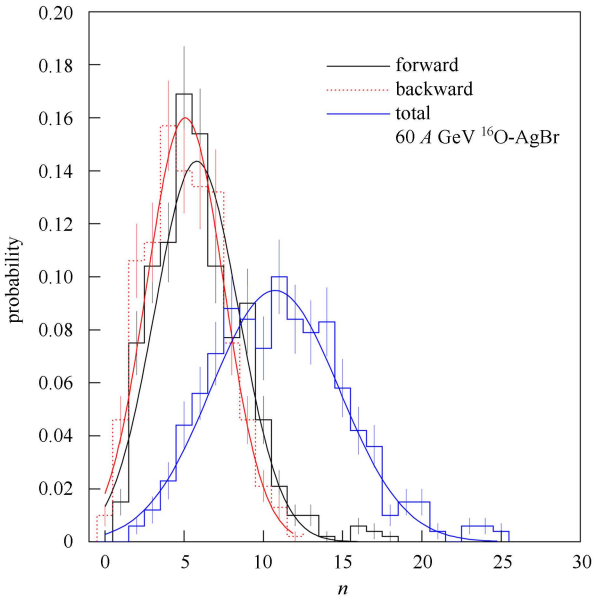

Fig. 3. (color online) Multiplicity distributions of target evaporated fragments emitted in 60 A GeV ^{16}O-AgBr interactions; the smooth curves are the results from the Gaussian fitting.

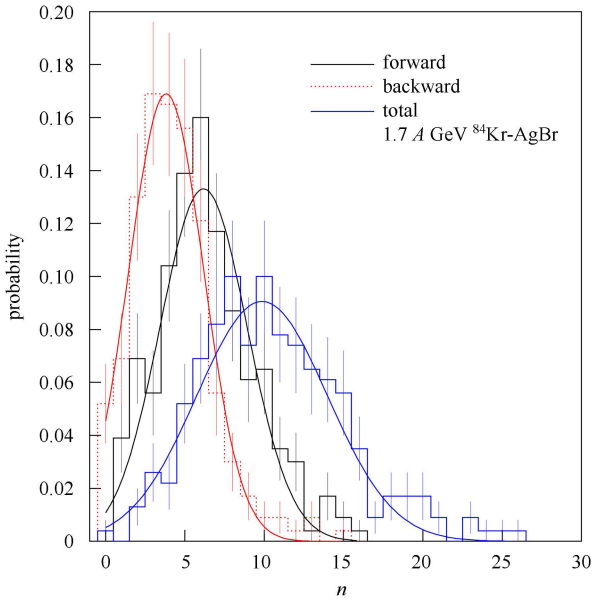

Fig. 4. (color online) Multiplicity distributions of target evaporated fragments emitted in 1.7 A GeV ^{84}Kr-AgBr interactions; the smooth curves are the results from the Gaussian fitting.

Equivalently, the multiplicity distribution can be studied using the moments of the distribution, which are given by

$$C_q=\frac{\langle n^q\rangle}{\langle n\rangle^q}=\frac{\sum_n n^q P_n}{(\sum_n nP_n)^q}, \quad (1)$$

where q is a positive integer called the order of the moment and P_n is the probability of producing or emitting n particles. Here

$$\langle n^q\rangle=\sum_n n^q\frac{\sigma_n}{\sigma_{\rm inel}}, \quad (2)$$

where σ_n is the partial cross section for producing or emitting a state of multiplicity n, $\sigma_{\rm inel}$ is the total inelastic cross-section and $\langle n\rangle$ is the average multiplicity.

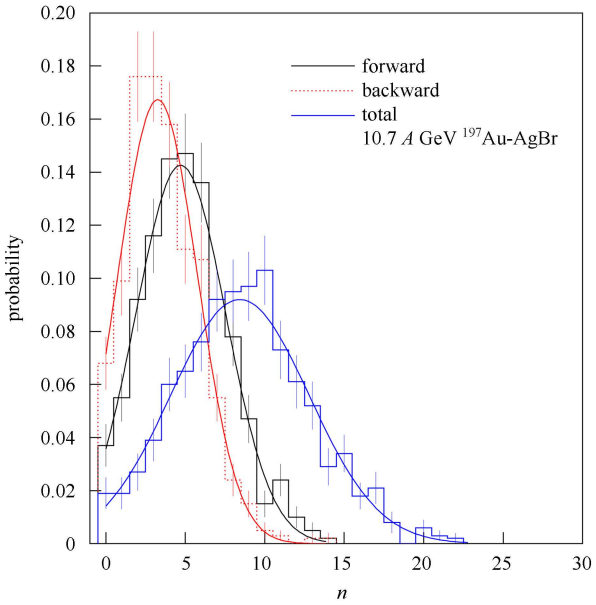

Fig. 5. (color online) Multiplicity distributions of target evaporated fragments emitted in 10.7 A GeV ^{197}Au-AgBr interactions; the smooth curves are the results from the Gaussian fitting.

The multiplicity moments, sometimes called the reduced C moments, can be used to describe the properties of multiplicity distributions, e.g. as a function of the projectile energy in the center-of-mass frame or in the laboratory frame. In practice, only the first few moments can be calculated with reasonable accuracy, due to the limited statistics. Table 3 presents the multiplicity moments of target evaporated fragments emitted in 12 A GeV ^{4}He, 3.7 A GeV ^{16}O, 60 A GeV ^{16}O, 1.7 A GeV ^{84}Kr and 10.7 A GeV ^{197}Au -induced AgBr interactions, with the corresponding results in Ref. [3] also included. In both the hemispheres, for all the interactions, the multiplicity moments increase with the order of the moment q, and the second order multiplicity moments are energy independent over the entire energy range in the forward and backward hemispheres. In the backward hemisphere, multiplicity moments up to the third order are also energy independent for all the interaction. The energy-independent behavior of multiplicity moments may hint at the existence of KNO scaling, which is an energy independent scaling law of multiplicity distribution proposed by Koba, Nielsen and Olesen [6].

Table 3. Values of the multiplicity moments of target evaporated fragments in the forward and backward hemispheres for different type of nucleus-AgBr interactions.

beam	forward hemisphere			backward hemisphere			reference
	C_2	C_3	C_4	C_2	C_3	C_4	
12 *A* GeV He	1.38±0.06	2.35±0.17	4.67±0.24	1.41±0.06	2.43±0.17	4.87±0.29	this work
3.7 *A* GeV O	1.28±0.09	1.94±0.21	3.35±0.25	1.31±0.09	2.02±0.22	3.52±0.32	this work
60 *A* GeV O	1.22±0.10	1.74±0.23	2.87±0.25	1.23±0.10	1.72±0.21	2.65±0.26	this work
1.7 *A* GeV Kr	1.24±0.16	1.77±0.34	2.84±0.40	1.36±0.22	2.30±0.60	4.66±0.84	this work
10.7 *A* GeV Au	1.29±0.11	1.94±0.24	3.25±0.34	1.39±0.13	2.32±0.35	4.50±0.60	this work
3.7 *A* GeV C	1.32±0.09	2.12±0.12	3.90±0.21	1.26±0.03	1.86±0.12	2.95±0.32	[3]
14.5 *A* GeV Si	1.20±0.07	1.63±0.14	2.45±0.28	1.23±0.04	1.79±0.13	2.98±0.47	[3]
60 *A* GeV O	1.19±0.08	1.63±0.15	2.51±0.37	1.24±0.05	1.83±0.15	3.03±0.63	[3]
200 *A* GeV S	1.30±0.05	1.94±0.18	3.16±0.46	1.30±0.08	2.06±0.21	3.92±0.81	[3]

Table 4. Values of entropy, reduced entropy and scaled variance of target evaporated fragments in the forward and backward hemispheres for different type of nucleus-AgBr interactions.

beam	forward hemisphere			backward hemisphere			reference
	S	$S/\langle n\rangle$	w	S	$S/\langle n\rangle$	w	
12 *A* GeV He	2.38±0.12	0.52±0.03	1.76±0.02	2.20±0.09	0.60±0.03	1.50±0.01	this work
3.7 *A* GeV O	2.54±0.25	0.42±0.04	1.72±0.02	2.29±0.18	0.51±0.04	1.39±0.01	this work
60 *A* GeV O	2.36±0.27	0.39±0.05	1.32±0.04	2.28±0.23	0.45±0.04	1.15±0.01	this work
1.7 *A* GeV Kr	2.49±0.44	0.39±0.07	1.51±0.02	2.26±0.37	0.54±0.08	1.52±0.07	this work
10.7 *A* GeV Au	2.38±0.23	0.47±0.05	1.46±0.01	2.17±0.20	0.60±0.06	1.41±0.02	this work
3.7 *A* GeV C	2.54±0.11	0.39±0.01	2.12±0.03	2.30±0.20	0.43±0.01	1.40±0.02	[3]
14.5 *A* GeV Si	2.24±0.14	0.38±0.02	1.15±0.01	2.18±0.19	0.44±0.02	1.12±0.02	[3]
60 *A* GeV O	2.32±0.14	0.35±0.01	1.25±0.02	2.21±0.11	0.43±0.01	1.25±0.03	[3]
200 *A* GeV S	2.31±0.16	0.43±0.03	1.60±0.05	2.03±0.12	0.45±0.01	1.35±0.03	[3]

It is known that the probability of multiplicity can be used to evaluate the entropy of the produced particles. The entropy of the produced particles can be calculated using the formula defined by Wehrl [7] as

$$S=-\sum_n P_n \ln P_n. \tag{3}$$

Here P_n is the probability of having n produced particles in the final state such that $\sum P_n=1$ for any phase space interval. The parameter entropy is related to the fractal dimension - to be more specific, the information dimension [8, 9]. The entropy is invariant under an arbitrary distortion of multiplicity scale; in particular, if a sub-sample of particles, such as charged particles, is chosen. Using Eq. (3), we have calculated the entropy and the reduced entropy ($S/\langle n\rangle$), i.e. the ratio of the entropy to average multiplicity of target evaporated fragments in the forward and backward hemisphere for all the nucleus–nucleus interactions we have investigated. Table 4 presents our results together with the results in Ref. [3]. It is found that the entropy value of the target evaporated fragments emitted in the forward hemisphere is greater than that emitted in the backward hemisphere, and the values of entropy remain almost energy independent in both hemispheres.

Finally, we want to evaluate the multiplicity correlation among the target evaporated fragments in the forward and backward hemispheres respectively. A useful measure of the fluctuation of any variable is the ratio of its variance to its mean value, so the variance of the multiplicity distribution can be used to measure the multiplicity fluctuations. In order to study the multiplicity fluctuations in high energy nucleus–nucleus collisions, we use a scaled variable w suggested by Ghosh et al. [3] such that

$$w=\frac{\langle n^2\rangle-\langle n\rangle^2}{\langle n\rangle}. \tag{4}$$

Multiplicity fluctuation is one aspect of a two-particle correlation function. The study of the scaled variance can very easily reveal the nature of the correlation among the produced particles. If the value of w is much greater than 1, it may be said that there is a strong correlation among the produced particles. In contrast, if the value of w is close to one, weak correlation is indicated. The scaled variance w of target evaporated fragments emitted in the forward and backward hemispheres for our investigated high-energy nucleus–nucleus collisions is presented in Table 4, with the corresponding values in Ref. [3] also shown in the table. It can be seen that the scaled variances of target evaporated fragments are close to one in both hemispheres for all the interactions, which suggests that there is a weak correlation in production of the tar-

get evaporated fragments in the forward and backward hemispheres.

4 Conclusions

The multiplicity distribution, multiplicity moment, scaled variance, entropy and reduced entropy of target evaporated fragments emitted in forward and backward hemispheres in 12 A GeV ^{4}He, 3.7 A GeV ^{16}O, 60 A GeV ^{16}O, 1.7 A GeV ^{84}Kr and 10.7 A GeV ^{197}Au -induced emulsion heavy targets' (AgBr) interactions have been investigated. It is found that the multiplicity distribution of target evaporated fragments emitted in forward and backward hemispheres can be fitted by a Gaussian distribution. The Gaussian fitting parameters are different between the forward and backward hemispheres for all the interactions, which may indicate that the nature of the emission of target evaporated particles differs between the two hemispheres. The multiplicity moments of target evaporated particles emitted in the forward and backward hemispheres increase with the order of the moment q, and the second-order multiplicity moments of the target evaporated fragments in both hemispheres are energy independent over the entire energy range for all the interactions. The scaled variance, a direct measure of multiplicity fluctuations, is close to one for all the interactions, which may show that there is a weak correlation among the target evaporated fragments. The entropy of target evaporated fragments emitted in the forward and backward hemispheres are the same within experimental errors.

We are grateful to the EMU-01 collaboration for supplying emulsion stacks.

References

1 Bowman J D, Swiatecki W J, Tsang C F. Abrasion and Ablation of Heavy Ions. Lawrence Berkeley Report: LBL-2908, 1973
2 Powell C F, Fowler P H, Perkins D H. The Study of Elementary Particles by the Photographic Method, Pergamon Press. London, New York: Paris, Los Angles, 1959. 432
3 Ghosh D, Deb A, Bhattacharyya S. Phys. Scr., 2011, **84**: 015201
4 ZHANG Dong-Hai, CHEN Yan-Ling, WANG Guo-Rong et al. Chin. Phys. C, 2015, **39**: 014001
5 Stocker H, Maruhn J A, Greiner W. Z. Phys. A, 1979, **293**: 173–179
6 Koba Z, Nielsen H B, Olesen P. Nucl. Phys. B, 1972, **40**: 317–334
7 Wehrl A. Rev. Mod. Phys., 1978, **50**: 221-260
8 Simak V, Sumbera M, Zborovski I. Phys. Lett. B, 1988, **206**: 159–162
9 Ghosh D. Roy J. Sengupta A G et al. Can. J. Phys., 1992, **70**: 667–669